Environmental Toxicology

WILEY

ENVIRONMENTAL TOXICOLOGY

RESEARCH ARTICLE OPEN ACCESS

Astaxanthin Alleviates Lung Injury by Regulating Oxidative Stress, Inflammatory Response, P2X7 Receptor, NF-κB, Bcl-2, and Caspase-3 in LPS-Induced Endotoxemia

Seckin Ozkanlar[1] | Yunusemre Ozkanlar[2] | Adem Kara[3] | Elif Dalkilinc[1]

[1]Department of Biochemistry, Faculty of Veterinary Medicine, Ataturk University, Erzurum, Turkey | [2]Department of Internal Medicine, Faculty of Veterinary Medicine, Ondokuz Mayis University, Samsun, Turkey | [3]Department of Genetics, Faculty of Science, Erzurum Technical University, Erzurum, Turkey

Correspondence: Seckin Ozkanlar (seckin.ozkanlar@atauni.edu.tr; seckinozkanlar@yahoo.com)

Received: 7 June 2024 | **Revised:** 7 October 2024 | **Accepted:** 16 January 2025

Keywords: anti-inflammatory | antioxidant | astaxanthin | P2X7 receptor | sepsis

ABSTRACT

Sepsis remains the leading cause of multiple-organ injury due to endotoxemia. Astaxanthin (ASTA), widely used in marine aquaculture, has an extraordinary potential for antioxidant and anti-inflammatory activity. Purinergic receptor (e.g., P2X7R) activation is a powerful signaling in the modulation of inflammation. The effect of ASTA was investigated on the regulation of oxidative stress, inflammatory response, apoptotic mediators, and P2X7R expression in the lung injury during lipopolysaccharide (LPS)-induced endotoxemia. Twenty-four rats were blocked into four groups as Control, LPS, ASTA, and LPS + ASTA. LPS was administered by intraperitoneal injection and ASTA by gavage. Blood and lung samples were taken 6 h after the administrations. The methods were ELISA, western blotting, histopathology, and immunohistochemistry. Sepsis was confirmed by the elevations of IL-1β, IL-6, IL-10, and TNF-α levels in bloodstream. Lung injury was determined by histopathological changes. There were increased P2X7R expression, malondialdehyde (MDA), IL-1β, TNF-α, nuclear factor kappa B (NF-κB), and Caspase-3 and decreased B-cell lymphoma 2 (Bcl-2) and glutathione (GSH) in the septic lung tissue ($p < 0.05$). ASTA treatment improved MDA, GSH, IL-1β, TNF-α, P2X7R, NF-κB, Caspase-3, and Bcl-2 levels and reduced P2X7R immunoreactivity and histological abnormalities in the lung ($p < 0.05$). The production of pro-inflammatory cytokines, oxidative stress, P2X7R expression, and apoptotic mediators in the lung is associated with LPS-induced endotoxemia. The ASTA administration appears to regulate the expressions of P2X7R, NF-κB, Bcl-2, and Caspase-3 improving the antioxidative and anti-inflammatory response of the lung tissue in sepsis, in vivo.

1 | Introduction

Sepsis is initiated by an infection activating a cascade of systemic response in inflammatory pathways which may progress to multiple-organ failure and mortality due to endotoxemia. Sepsis-related deaths are attributed to underlying diseases when mortality rates are compiled [1], as sepsis is not a specific disease but rather a syndrome [2]. Bacteria are the most common causes of sepsis by the activation of inflammatory response ranging from hyper-responsive to hypo-responsive states [3]. This systemic inflammatory response may lead to acute respiratory distress syndrome (ARDS) associated with an infection and/or endotoxemia [4]. During Gram-negative bacterial sepsis, lipopolysaccharide (LPS) stimulates toll-like receptor (TLR), and cell-surface receptors that trigger pro-inflammatory cascades, inflammation, and cell differentiation in many organs including the lung [1, 5]. LPS administration facilitates an endotoxemia model to evaluate organ damage such as acute lung injury (ALI) [6]. The mechanisms of organ damage in the early sepsis are mainly related with

the cytokine storm caused by intense inflammatory response [7, 8]. Therefore, identifying the signaling mechanisms of cell death is crucial to develop a novel therapeutic approach that inhibits the extrinsic and intrinsic cascades of apoptosis mediated by cytokine production and transcriptional regulators such as nuclear factor kappa B (NF-κB), Caspase-3, and B-cell lymphoma 2 (Bcl-2) in ALI [9] during sepsis which is one of the common causes of mortality worldwide [10].

Adenosine 3′-triphosphate (ATP) passes into the extracellular fluid when cell integrity disrupted that cause ion channel activation via purinergic receptor (P2X) signaling [11–13]. Purinergic signaling cascade may be one of the essential components to the response against pathogens. One of the most important generator of oxidants during sepsis is the reaction of phagocytes in the inflamed lung tissue that reduce the respiratory capacity [14] in which the leaking ATP into extracellular space exaggerates the generation of reactive oxygen species (ROS) and mitochondrial damage [15]. The P2X7 receptor (P2X7R) activation is known as a powerful response in the regulation of caspase inflammasome activation that requires priming of macrophages [16] associated with immunology and inflammation [17, 18]. Recently, we have demonstrated that LPS-induced sepsis causes P2X7R overexpression, proinflammatory cytokine overproduction, and oxidative stress generation in the lung [19]. A previous report has also shown the similar findings in the liver [20]. A decrease in inflammatory cells infiltration and cytokine production has been reported in the liver of P2X7R knockout mice suggesting P2X7R deletion attenuates organ damage in sepsis [21]. Therefore, the activation of P2X7Rs has been suggested to involved in the NF-κB transcription that may need to signaling mechanisms such as ROS generation and caspase activation [22] while P2X7R-induced caspase activation and cytokine production may require NLRP3 and NF-κB signaling following TLR stimulation in inflammation [23, 24]. Additionally, P2X7R antagonism has been shown to ameliorate renal dysfunction [25] and alleviate oxidative stress of lung in sepsis [19].

Astaxanthin (ASTA), produced from microalgae and widely used in marine aquaculture, is a unique ketocarotenoid red pigment [26] with its outstanding potential for antioxidant, anti-inflammatory, anti-atherosclerotic, and antitumor activity in the prevention of many diseases [26–28]. ASTA has high bioavailability against oxidative stress and inflammatory reactions [29]. In addition, ASTA administration downregulates P2X7R expression in brain and improves neuroinflammation by regulating the ATP-P2X7R signaling [30]. In ALI, ASTA treatment has a protective effect against the disease development with the ability to inhibit oxidative/nitrative stress [31] and to attenuate lung edema, inflammatory cells infiltration, and ferroptosis [32]. Therefore, the modulation of the signaling pathway associated with the P2X7R activation at the early phase of the inflammatory response would facilitate the treatment of septic organ damage [21, 25, 33]. This study investigates the effects of ASTA administration on the regulation of P2X7R expression, cytokine response, oxidative stress markers, apoptotic mediators, and histopathological changes with regard to inflammatory-apoptotic pathway in the septic lung injury in a murine model of sepsis.

2 | Materials and Methods

2.1 | Animals and Study Design

The animals recruited in this study were 3-month-old male Sprague Dawley rats weighing between 200 and 300 g. All rats were accommodated with standard breeding conditions in the medical experimental research unit of the university. Twenty-four rats were blocked into four groups having six animals in each. Control group received intraperitoneal (i.p.) 0.5 mL of sterile saline solution (0.09%). LPS group received i.p. 4 mg/kg LPS (L2880, *Escherichia coli* O55:B5, Sigma, USA). Animals in ASTA group received oral 40 mg/kg ASTA (Astaxanthin, SML0982, Sigma, USA) by gavage. Animals in LPS + ASTA group received i.p. 4 mg/kg LPS plus oral 40 mg/kg ASTA by gavage. The doses used in this study were investigated according to the previous reports for LPS [34, 35] and ASTA [36, 37] administrations. Sterile saline solution (0.09%) was used for the dilutions of LPS and ASTA. The schedule of the experiment was 6 h of duration from the LPS induction and drug administrations through the sample collection in which the animals were allocated into the labeled cages for each group. This experimental design had an approval from the local ethics committee for animal researches (HADYEK, decision no 2022/97). This study was done according to the international ethical standards of the guide for the care and use of laboratory animals.

2.2 | Blood and Lung Tissue Sampling

Blood and lung tissue samples were obtained 6 h after the LPS induction to examine the acute effects of drug administration in an ALI model [19, 38]. All animals in control and sepsis groups were sedated by inhalation of 5% sevoflurane (Sevorane, Abbott GmbH & Co.KG, Germany) anesthesia to lessen the systemic effects of anesthesia [39, 40]. Approximately 7–8 mL blood was sampled into blood tubes (Becton Dickinson Co. USA), and the rats were sacrificed by cervical dislocation. Lung tissue samples were removed into the sterile petri dishes for biochemical analysis. Lung tissues were also sampled into freshly prepared 10% formaldehyde solution and embedded into paraffin blocks for histological examinations. The right and the left lung lobes were sampled for both biochemical and histopathological examinations to evaluate whole lung in the analyses. Sera samples were separated into Eppendorf tubes for each animal following the blood centrifugation at 3500 rpm (Hettich 38R, Hettich Zentrifugen, Tuttlingen, Germany) at 4°C for 10 min. The Eppendorf tubes for sera samples and the petri dishes for lung tissues were stored at −80°C for further assays.

2.3 | Determination of IL-1β, IL-6, IL-10, TNF-α, and Caspase-3 in Blood Serum

Serum cytokine and Caspase-3 levels were analyzed by solid phase ELISA method. ELISA kits were used to analyze cytokines (TNF-α [201-11-0765], IL-6 [201-11-0136], IL-10 [201-11-0109], and IL-1β [201-11-0120]) and Caspase-3 (201-11-5114, Shanghai Sunred Biotechnology, China). Absorbances were measured by a microplate spectrophotometry (BioTek, μQuant, USA) at 450 nm.

2.4 | Determination of Oxidative and Antioxidative Status in Lung Tissue

MDA, glutathione (GSH), and superoxide dismutase (SOD) levels were measured by ELISA method according to manufacturers' instructions after tissue preparation. First, liquid nitrogen was added onto the lung tissue. Then, the tissue was lysed with a tissue lyser (Tissue Lyser II, Qiagen, Germany) for 3 min and the sample with PBS at pH 7.4 was homogenized for 20 s at 30 Hz. Supernatants were obtained by centrifugation at 3000 rpm. These supernatants were then analyzed using commercial kits (MDA [201-11-0157], GSH [201-11-5137], and SOD [201-11-0169], Shanghai Sunred Biotechnology, China) and tissue protein (BR05, Bradford Reagent, EchoTech Biotechnology, Turkey). The absorbances were read at 450 nm for MDA, GSH, and SOD and at 595 nm for tissue protein using a microplate spectrophotometry (BioTek, μQuant, USA).

2.5 | Determination of Bcl-2, Caspase-3, NF-κB, P2X7R, Il-1β, and TNF-α in Lung Tissue

Relative protein expressions in lung tissue samples were determined by Western blotting. The tissues were weighed and liquid nitrogen was used for crushing. The samples were treated with RIPA buffering with supplementation of protease and phosphatase inhibitors. The homogenization was performed by Qiagen Tissue Lyser System at 30 Hz for 20 s. The total protein content of lung tissue was quantified using protein assay kit (Pierce BCA, Thermo Scientific, USA). Total protein (30 μg) was separated into 10% SDS-PAGE based on molecular weights and loaded to PVDF membranes. The blockage of membranes was performed using 5% w/v bovine serum albumin for 90 min. The membranes were incubated with primary antibodies (IL-1β [sc-52 012], TNF-α [sc-52 746], Caspase-3 [sc-56 053], Bcl-2 [sc-7382], NF-κB-p65 [sc-109], and Beta-actin [sc-47 778], Santa Cruz Biotechnology, USA; P2X7R [11144-1-AP], Proteintech Group, USA) at 4°C for about 15 h. After washing by Tris-buffered saline with Tween, the membranes were incubated for 90 min with secondary antibodies (sc-2004/sc-2005, Santa Cruz Biotechnology, USA,) conjugated to horseradish peroxidase (TP-125-HL, Thermo Fisher Scientific, USA). Finally, chemiluminescence visualization of protein bands was achieved by an enhanced Western ECL substrate (3405, Thermo Fisher Scientific, USA) for software evaluation (Image Lab, Bio-Rad, USA).

2.6 | Histopathological Evaluation

The lung tissue samples were fixed in 10% formaldehyde solution. The tissues were embedded in paraffin blocks and 5-μm-thick tissue sections were cut by using a microtome (Leica Microsystems, Wetzlar, Germany). The lung tissue samples were stained with Crossman's Modified Triple Staining and serial photographs of the sections were taken by a camera-attached light microscope (Nikon Eclipse i50, Tokyo, Japan). Pulmonary edema, vascular and alveolar structures, and bronchiolar changes were histopathologically examined in 5-μm lung tissue sections. The examinations were then assigned to 0 for normal, 1 for mild, 2 for moderate and 3 for severe according to the evaluation criteria [41]. Briefly, the main evaluation criteria were based on intravascular occlusion, inflammatory cell infiltration (leukocytes), pulmonary obstruction, alveolar septum thickening, amorphous material, and bronchiole epithelium detachment.

2.7 | Immunohistochemical Analysis

The paraffin blocks of the lung tissues were sectioned at a thickness of 4 μm and placed on poly-lysine slides. The sections were then treated with a series of xylol and alcohol washes, followed by a wash with phosphate-buffered saline containing 3% H_2O_2 for 10 min that inactivates endogenous peroxidase. To expose antigens, citrate solution in pH 6.0 was applied to these sections at 600 watts for 4 × 5 min. Protein blocking solution was applied to the tissues before the incubation with the primary antibody of P2X7R (11144-1-AP, Proteintech Group, USA) in a 1:200 dilution at +4°C for about 15 h. The secondary antibody was applied according to the manufacturer's instructions (Large Volume Detection System, Anti-Polyvalent, HRP, TP-125-HL, Thermo Fisher Scientific, USA). The chromogen 3,3′-diaminobenzidine (DAB) was used as (DAB, Thermo Fisher Scientific, USA). The slides were stained with Mayer's hematoxylin and mounted with Entellan. A blind examination was performed on random areas over the slides by the same histopathologist.

2.8 | Stereological Immunoreactivity Analysis

To verify the specificity of staining for immunohistochemistry, the same procedures were performed on each section with negative controls, substituted PBS for primary antibody. The immunohistochemical reactions of tissue slides were evaluated by a light microscope (Bx53, Olympus, Japan), followed by photography. Semiquantitative analyses assessed the degree of cellular immunoreactivity across all groups. The values of numerical density were determined in immunoreactive cells of lung tissues and assessed by a stereology workstation. This workstation consists of an adapted light microscope (DM4000B, Leica Microsystems, Germany) and a stereology software (Stereo-Investigator 9.0, Microbrightfield, USA). The fractionator principle was used for sampling the sections. To ensure an accurate detection, the calculation of cells was determined with 40X Apo objective of Leica Plan (NA = 1.4).

2.9 | Statistical Analysis

A software program (SPSS 25.0, IBM, USA) was used for statistical comparison. The homogeneity of variance test showed a normal distribution of the data with 95% confidence interval. One-way ANOVA with Tukey's post hoc test was used to analyze multiple comparisons. The subset for the significance of the p value was 0.05 alpha level. Statistical significance levels were presented as $^{*}p < 0.05$, $^{**}p < 0.01$, and $^{***}p < 0.001$. The data were presented as mean ± SEM for the biochemical variables and mean ± SD for the histopathological scoring.

3 | Results

3.1 | LPS Induction Causes Severe Sepsis Through Cytokine Overproduction in Bloodstream

There were severe increases in IL-1β, IL-6, IL-10, TNF-α, and Caspase-3 levels in the LPS group compared with the Control group in sera samples ($p < 0.001$) while there was no statistical difference in between Control and ASTA groups ($p < 0.05$). ASTA administration decreased the levels of IL-10, TNF-α, and Caspase-3 in the LPS + ASTA group compared with the LPS group ($p < 0.001$), and the levels were not different from the Control group ($p > 0.05$). The levels of IL-1β and IL-6 in the LPS + ASTA group were moderately higher than the Control group ($p < 0.05$) although the levels were not different from the LPS group ($p > 0.05$). Mean serum values of cytokines and Caspase-3 levels in the groups are presented in Figure 1.

3.2 | LPS Induction Causes Severe Oxidative Stress in Lung Tissue That Can be Prevented by ASTA Administration

The level of MDA in LPS group was high compared to Control and ASTA groups ($p < 0.001$) with no difference in between Control and ASTA groups ($p < 0.05$) in lung tissue. The MDA level was reduced by ASTA administration in LPS + ASTA group compared to LPS group ($p < 0.01$) although the level was moderately higher than Control and ASTA groups ($p < 0.05$). GSH level decreased in LPS group compared to Control ($p < 0.01$) and ASTA ($p < 0.001$) groups. ASTA treatment improved GSH level in LPS + ASTA group compared to LPS group ($p > 0.01$) with no difference in between Control and ASTA groups ($p > 0.05$). SOD level did not differ in Control, LPS, and ASTA groups ($p > 0.05$) while it was higher in LPS + ASTA group than Control ($p < 0.05$) and LPS ($p < 0.01$) groups with an increasing tendency compared with ASTA group ($p = 0.059$). Oxidative and antioxidative status in the lung tissue is presented in Figure 2.

3.3 | Histopathological Findings

Figure 3 shows the mean scores for histopathological evaluation of the lung tissues in the groups. Vascular, alveolar, bronchiolar, and mean histopathological score values of lung tissues were significantly higher in the LPS group than in the Control group ($p < 0.05$). Significant decreases in the score values were determined in the AST + LPS group compared to LPS group ($p < 0.05$) while the score values were high in the AST + LPS group compared to Control ($p < 0.05$). Histopathological illustrations of lung tissues representative for all groups are shown in Figure 4.

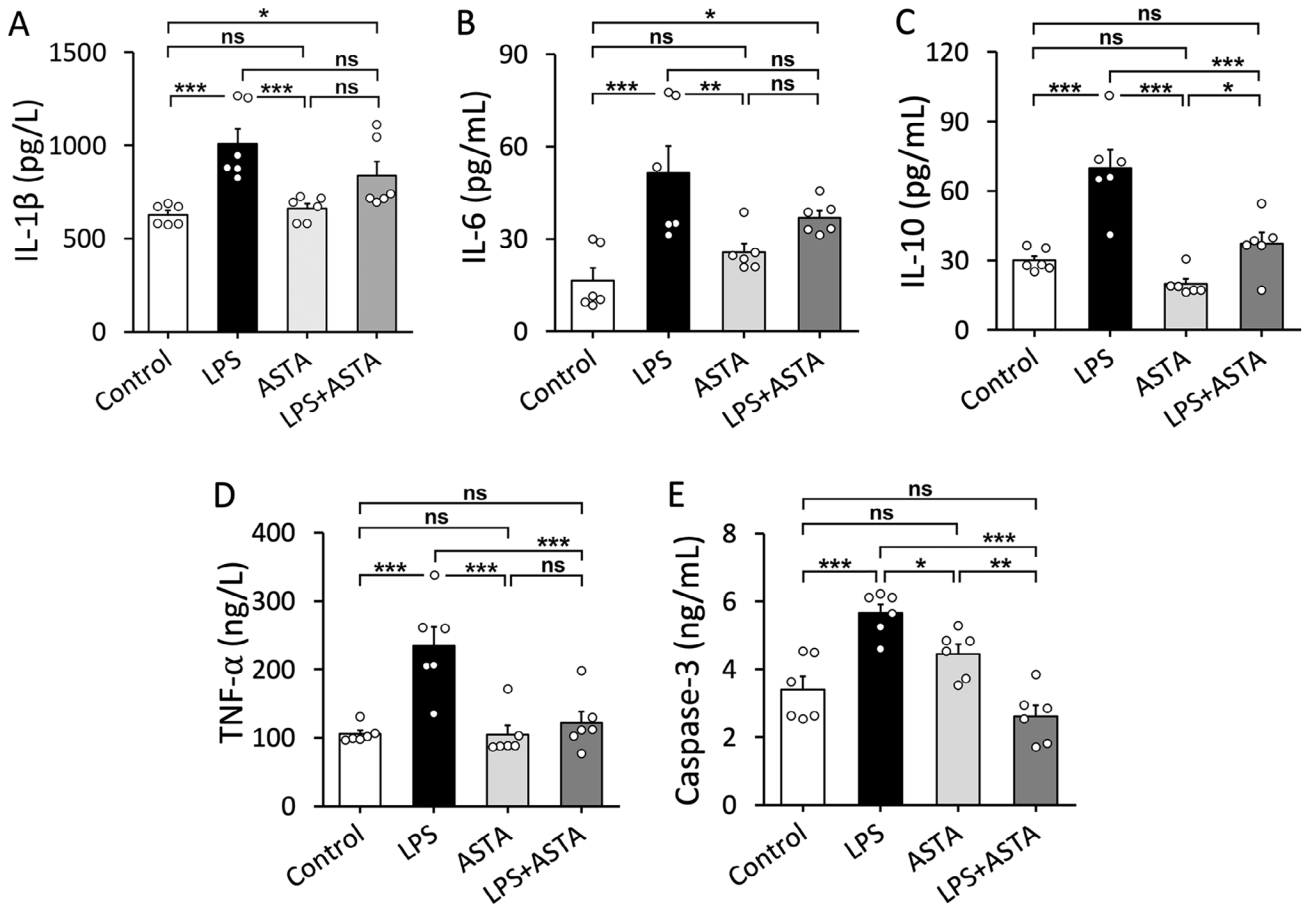

FIGURE 1 | Cytokine and Caspase-3 levels in sera samples. Note that the levels of IL-1β (A), IL-6 (B), IL-10 (C), TNF-α (D), and Caspase-3 (E) are higher in LPS group than in Control. ASTA administration decreases IL-10, TNF-α and Caspase-3 levels in LPS + ASTA group compared with LPS group. The levels of IL-1β and IL-6 in LPS + ASTA group were moderately higher than the Control group. Bars are mean ± SEM. Scatterplots are individual values for each animal. *$p < 0.05$; **$p < 0.01$; ***$p < 0.001$; ns, no significant ($p > 0.05$).

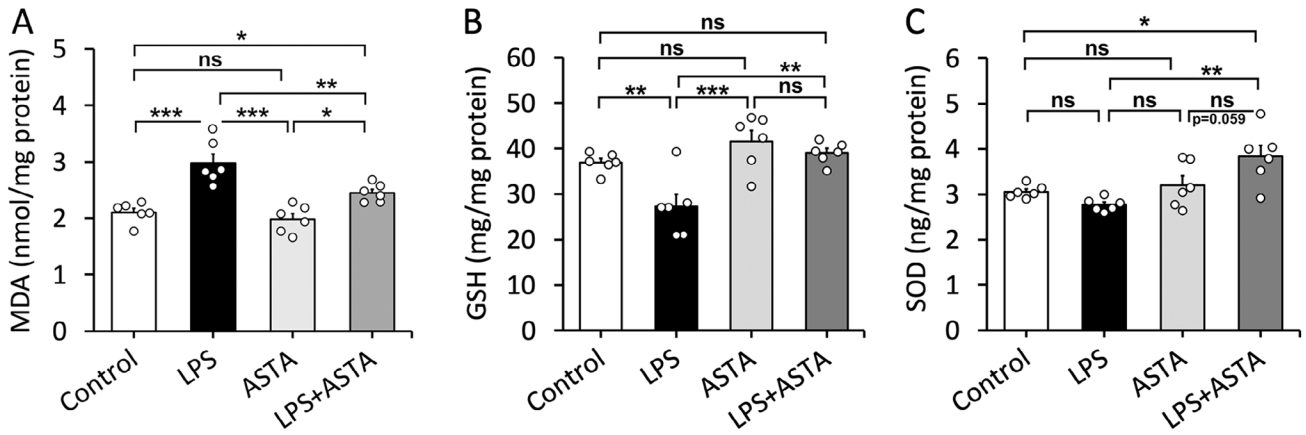

FIGURE 2 | Oxidative and antioxidative status of lung tissue. Note that the LPS administration increases the MDA level (A) and decreases the GSH level (B). The level of SOD (C) in LPS group is not statistically different from Control group. ASTA administration decreases MDA and increases GSH and SOD in LPS + ASTA group compared with LPS group. Bars are mean ± SEM. Scatterplots are individual values for each animal. $^{*}p < 0.05$; $^{**}p < 0.01$; $^{***}p < 0.001$; ns, no significant ($p > 0.05$).

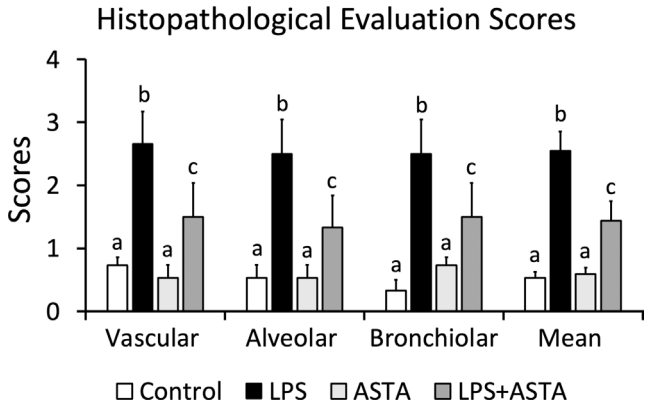

FIGURE 3 | Histopathological evaluation scores of the lung tissues in all groups. The scores were evaluated based on the findings of vascular, alveolar, and bronchiolar features. Results are shown as mean ± SD. Statistical differences among groups are shown with different letters ($p < 0.05$, at least).

3.4 | Immunohistochemical and Immunoreactivity Findings

Immunohistochemical staining of lung tissues incubated with P2X7R primary antibody is shown in Figure 5. Immunoreactivity was significantly increased in LPS group ($p < 0.05$) while slight immunoreactivities were determined in the lung tissues in Control and AST groups. There was a decrease in immunoreactivity in the AST + LPS group compared to LPS group ($p < 0.05$) but the score value of AST + LPS group was still higher than the score values of Control and AST groups ($p < 0.05$). The stereological immunoreactivity results are presented in Table 1.

3.5 | Western Blot Analysis Findings

The relative protein expression of Bcl-2 was low in LPS group compared to Control, ASTA, and LPS + ASTA groups ($p < 0.05$). The expression levels of Caspase-3, NF-κB-p65, P2X7R, IL-1β, and TNF-α in LPS group were significantly higher than in Control, ASTA, and LPS + ASTA groups ($p < 0.05$). The expression levels were improved in LPS + ASTA group compared to LPS group ($p < 0.05$) having a similarity with the expression levels of Control and ASTA groups ($p > 0.05$). The band images and band analyses in lung tissue of all groups are presented in Figure 6.

4 | Discussion

In this study design, the severe cytokine overproduction in bloodstream confirms systemic inflammatory response that is indicative to sepsis as a result of endotoxemia following the intraperitoneal administration of LPS. The histopathological alterations and inflammatory cell infiltration in the lung tissue demonstrate the ALI during endotoxemia. Sepsis-induced ARDS could arise from pulmonary or extrapulmonary infections resulting in ALI characterized by pulmonary inflammation [42, 43]. The excessive inflammatory response may cause tissue damage in sepsis while inflammatory regulation is required to accelerate the immunomodulation of inflammation. The immune response is regulated by interrelating reactions between pro- and anti-inflammatory responses [10] while sepsis may progress to life-threatening organ dysfunction or damage in a particular condition of dysregulated host response [3]. Therefore, the severity of inflammatory response demonstrates the severity of sepsis and tissue damage. In the current study, the inflammatory response of the lung caused by extrapulmonary *E. coli* LPS have been improved by the ASTA treatment through the regulation of ROS products, P2X7R expression, pro-inflammatory cytokine response, and apoptotic and anti-apoptotic mediators.

The antioxidant activity of ASTA in lung diseases is mostly associated with its supreme capacity for the absorbance of oxygen radicals (e.g., up to 500 times more effective than α-tocopherol), standing out from other antioxidants having a superior activity [28, 44]. During oxidative stress, generation of ROS produces lipid peroxidation that is recognized by pattern recognition receptors leading to DNA damage [45]. The lipid peroxidation product MDA is derived from superoxide radicals responding to oxidative stress and cell injury. ASTA treatment reduces ROS formation and oxidative stress occurrence [46] ameliorating

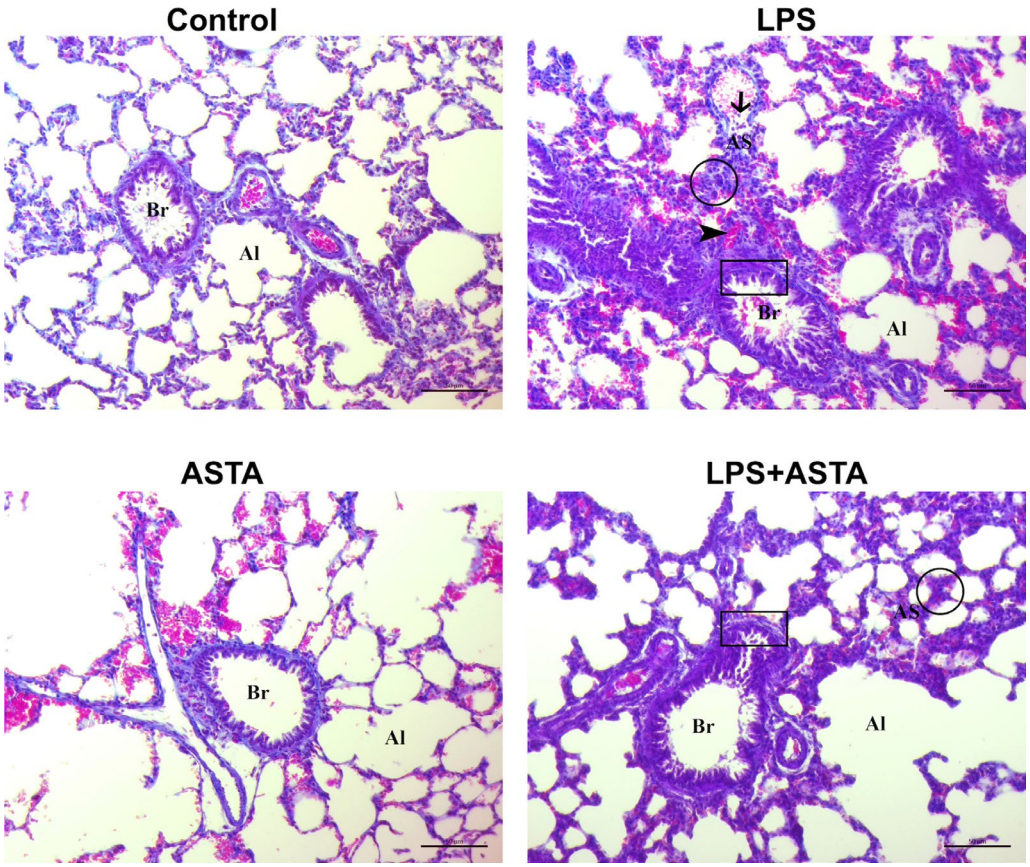

FIGURE 4 | Histopathologic illustration of lung tissues in the groups (Crossman's modified triple staining, magnification 200×). Al, alveoli; arrow head, alveolar hemorrhage; AS, alveolar septa; Br, bronchiole; circle, thickness in alveolar septa; square, detachment of the bronchial epithelium; open arrow, infiltration of inflammatory cells (leukocytes).

DNA damage and apoptosis reducing Caspase-3 activation [47] in the airway epithelium. ASTA suppresses ROS production and lipid peroxidation activity, upregulates antioxidant enzyme SOD, and inhibits cytokines (e.g., IL-1β) in LPS-induced dendritic cells providing a strong antioxidant protection for inflammatory control in sepsis [48]. A recent study has reported that ASTA improves the levels of MDA and GSH in the lung injury [49]. In accordance with previous reports, the findings seen in the treatment group indicate that the oxidative stress of the septic lung tissue can be alleviated by ASTA administration by decreasing MDA level along with an increase in GSH level. In addition, the P2X7R signaling can influence the production of lipid mediators in alveolar macrophages [50] through the regulation of signaling cascade and radical scavenging [51]. P2X7R antagonism reduces the cytokine production and ROS generation [52], suggesting that ROS may involve in the P2X7R-mediated cytokine overproduction [53]. Besides, we have recently determined that P2X7R antagonism may alleviate the oxidative stress of the lung tissue in LPS-induced sepsis in rats [19]. Thus, the current data demonstrate that ASTA treatment may alleviate lung injury through the downregulation of the P2X7R-mediated pathway that may possibly contribute to reduce the MDA level and to increase the GSH level boosting the antioxidative and anti-inflammatory responses of the lung.

Healthy tissues strictly regulate ATP release from cells to maintain the concentration low by extracellular ATP/ADPases although ATP may act as an endogenous danger signal released from injured cells into extracellular fluid that triggers inflammatory reactions to maintain immunity through purinergic signaling [12, 54]. When cell integrity disrupted, extreme amount of extracellular ATP interacts with the cell surface receptors (e.g., P2X7Rs) by mediating the inflammation and fibrosis in tissues including the lung [54] that may result in the activation of signaling cascades by inducing apoptosis [12, 13]. Ligand-gated ion channel P2X7 receptor has a significant role as a signal to activate inflammasomes inducing the productions of cytokine and ROS [12] while it has an immunoregulatory function [55]. Accordingly, P2X7R overexpression and ROS production (i.e., MDA) have been observed in the septic lung tissue which may involve in the inflammatory response during sepsis as seen in the animals given LPS, herein. There were increases in the expressions of P2X7R, NF-κB, and Caspase-3 and a decrease in Bcl-2 in the lung tissues of sepsis group. The Caspase-3 level increased in both lung and blood. Signaling mechanism and apoptosis are paired with the production of cellular pro-inflammatory/lipid mediators and the accumulation of activated neutrophils and macrophages into the lung tissue as the pathogenesis of lung injury is regulated by the transcriptional factors such as Caspase-3 and NF-κB [9]. The apoptosis cascade starts with different initial caspase signals and converges at the same final executor and effecter Caspase-3 that induces cell death in sepsis [56] in which apoptotic pathway could also be regulated by Bcl-2 family proteins in pulmonary diseases [57]. In addition, NF-κB serves as a pivotal mediator in response to inflammation by activating cytokines, adhesion molecules, cell proliferation, morphogenesis,

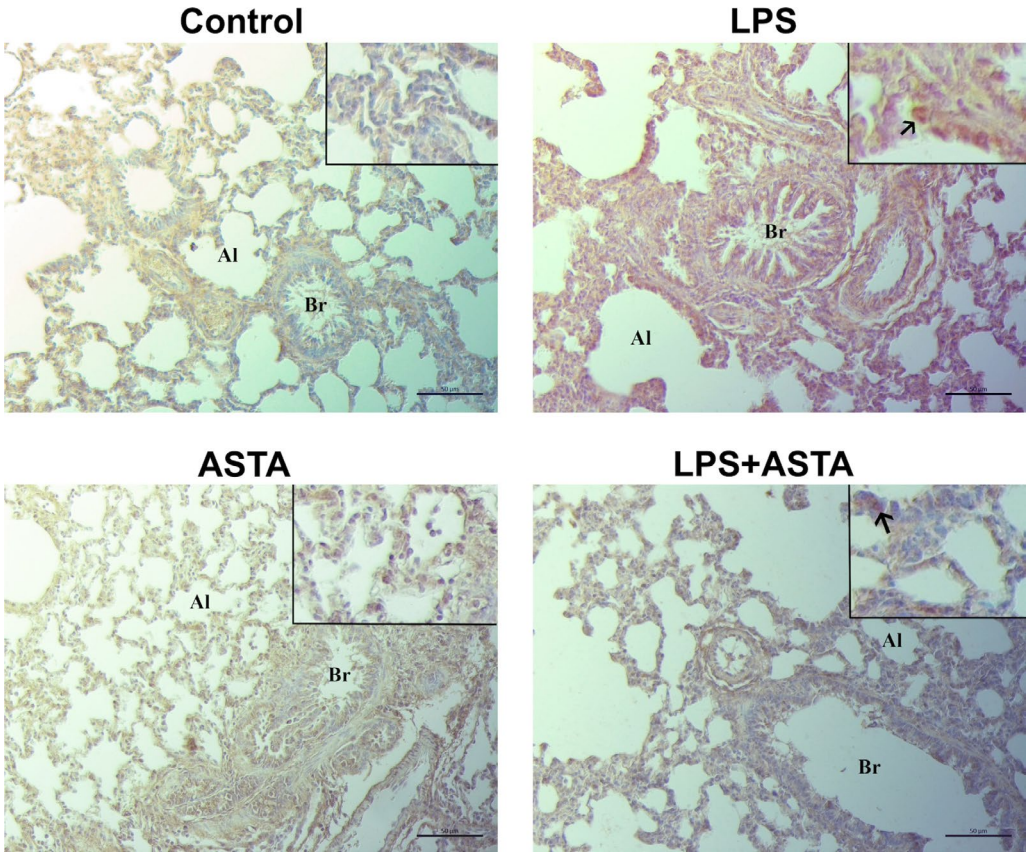

FIGURE 5 | Immunohistochemical staining of lung tissues with anti-P2X7R antibody in the groups (Avidin–biotin staining, magnification 200×). Br, bronchiole; Al, alveoli; arrows, immune reactive cells.

differentiation, and apoptotic changes [58]. A recent study found that P2Y2R and P2X7R activations increase adhesion of monocytes to endothelial cells inducing an upregulation of P2Y2R-P2X7R–mediated signaling, inflammasome activation, IL-1β release, and NF-κB signaling in mesenteric endothelial cells from peritoneal cavity [59]. Therefore, the P2X7R signaling, IL-1β release, and NF-κB activation may be one of the essential signaling pathways for the regulation of inflammatory response in lung injury during endotoxemia induced by intraperitoneal LPS.

The fact that the antagonism of P2X7Rs has attenuated the septic lung injury [33] indicates a strong evidence for the therapeutic targeting of the P2X7Rs [18]. The P2X7R positively regulates NF-κB activation and induces a rapid activation of caspases leading to apoptotic cell death [60]. The regulation of P2X7/NF-κB pathway prevents apoptosis improving the antioxidative and anti-inflammatory activity of myocardial cells [61]. P2X7R blockade mediates pyroptotic inflammation through the signaling pathway of NF-κB/NLRP3/Caspase-1 that promotes P2X7-dependent NF-κB-p65 translocation in murine macrophages in *Vibrio vulnificus* infection, a Gram-negative bacterium [62]. Suppression of P2X7/NF-κB pathway may particularly contribute to the downregulation of pro-inflammatory cytokines in LPS-induced inflammatory response of the lung [63]. Therefore, inflammatory stimulation appears to trigger inflammasome, P2X7Rs, NF-κB, and caspase signaling, leading to cytokine production and cell apoptosis. ASTA has extraordinary potential for protecting the organism against respiratory diseases due to its outstanding protective effects for the regulation of oxidative and inflammatory response in the sepsis-induced lung injury [31, 48]. LPS evokes alveolar macrophage decompose via CD14 and P2X7R, inducing the release of cytokines as an initiator of neutrophil infiltration [64]. The staining of lung tissue revealed that ASTA treatment has reduced LPS-induced alveolar and bronchiolar damage inhibiting inflammatory cell infiltration. Thus, the results of this study suggest a critical pathway for the pharmacotherapy to reduce the lung inflammation by regulating ROS products, pro-inflammatory cytokines, and P2X7R signaling and apoptotic mediators during sepsis.

TABLE 1 | Immunoreactivity results of anti-P2X7R antibody in lung tissues.

Groups	P2X7R
Control	0.33 ± 0.51^{a}
LPS	4.33 ± 0.81^{b}
ASTA	0.33 ± 0.51^{a}
LPS + ASTA	2.83 ± 0.75^{c}

Note: Results are shown as mean ± SD. Statistical differences among groups are shown with different letters in the same column ($p < 0.05$, at least).

The putative role of molecular mechanisms of ASTA treatment for the modulation of oxidative stress and inflammatory response have been previously documented [29, 65, 66]. ASTA activates Nrf2 (nuclear factor erythroid 2–related factor 2) leading to the synthesis of antioxidant enzymes [65] and regulates

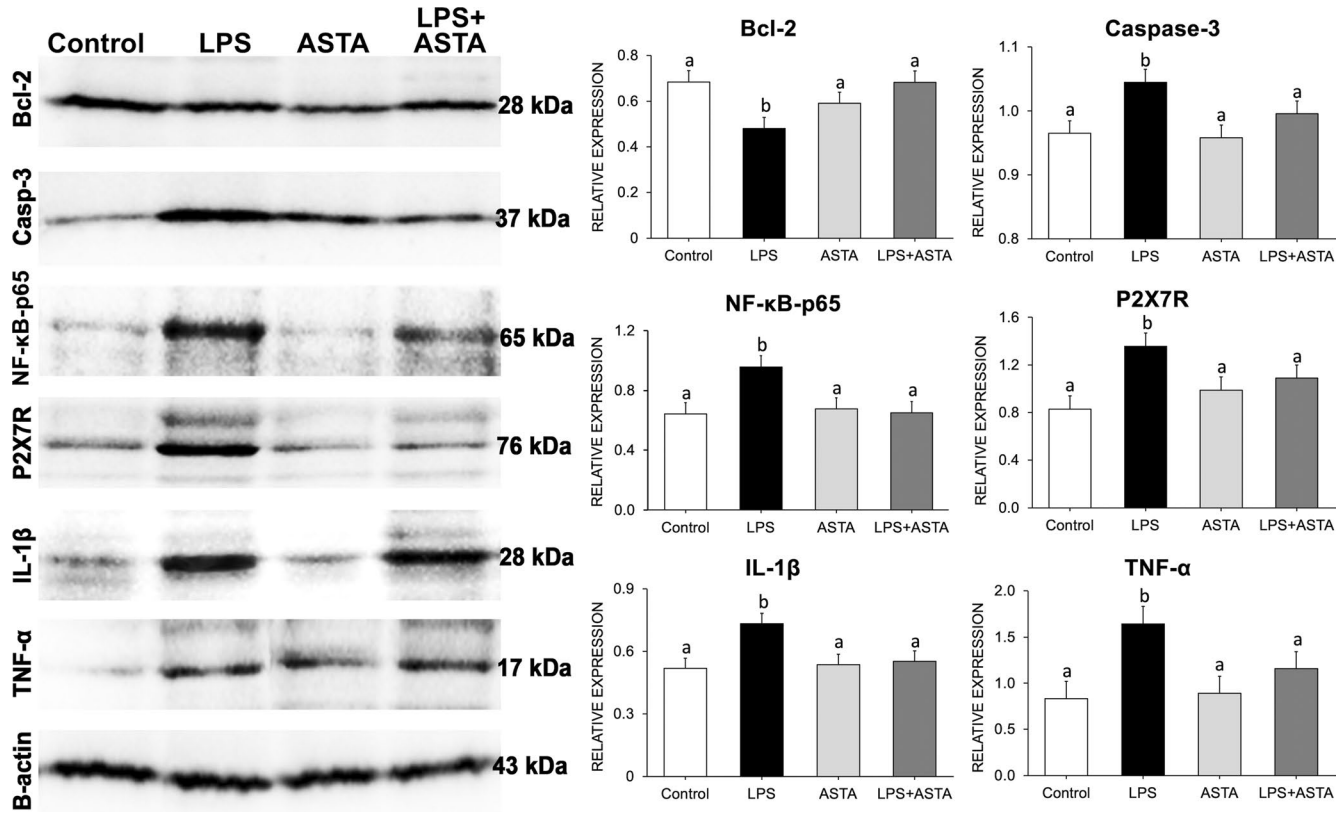

FIGURE 6 | Band images and relative protein expressions of lung tissues in the groups.

NF-κB and MAPK (mitogen-activated protein kinase) pathway associated with an anti-inflammatory effect on the lung diseases [67]. ASTA suppresses NF-κB in tuberculosis-associated lung injury [68] and non-small cell lung cancer [69]. ASTA modulates signaling pathways in LPS-induced inflammatory reactions in the lung [70]. It has been previously determined that LPS-induced apoptosis exhibits a decrease in the anti-apoptotic Bcl-2 and an increase in the pro-apoptotic Bax (Bcl-2 associated X) resulting in an elevation of the Bax/Bcl-2 ratio in lung tissue in the ALI [71]. There are many promising effects of ASTA treatment, for example, the inhibition of apoptosis through the regulation of NF-κB, Caspase-3, and Bcl-2 in lung diseases [67] as shown in the LPS + ASTA group. The anti-apoptotic mediator Bcl-2 inhibits the apoptosis not only in malignant cells and but also in normal cells [72]. In addition to the antioxidant effects of ASTA treatment, therefore, the findings indicate that the ASTA treatment may prevent the lung apoptosis during endotoxemia by the regulation of the apoptotic and anti-apoptotic mediators.

There are limitations of this study related with the LPS-induced endotoxemia that reflects Gram-negative bacterial sepsis without live bacteria. LPS model may exhibit a higher endotoxin resistance in murine models than human beings. On the other hand, pro-inflammatory cytokine release is one of the main characteristics of early sepsis which is associated with the organ damage among sepsis etiologies in which the Gram-negative bacteria are the leading causes of sepsis [3]. Further molecular studies are warranted to investigate the potential therapeutic effects of ASTA treatment on the regulation of oxidative stress and inflammatory-apoptotic pathway with regard to P2X7R signaling.

5 | Conclusion

The results of this study determine that the inflammation of lung tissue is triggered by LPS induced endotoxemia which apparently related with pro-inflammatory cytokine production (IL-1β and TNF-α), ROS generation (MDA), and purinergic signaling (P2X7Rs) leading to a susceptibility to cell damage by dysregulated apoptotic (NF-κB-p65 and Caspase-3) and anti-apoptotic (Bcl-2) mediators. ASTA administration appears to alleviate septic lung injury by regulating oxidative stress, P2X7R expression, cytokine production, and apoptotic mediators improving inflammation and apoptosis of the lung in LPS-induced endotoxemia, in vivo.

Author Contributions

Seckin Ozkanlar: conception, design, experiment, biochemical analysis, western blot, and manuscript writing and editing. **Yunusemre Ozkanlar:** conception, data analysis, and manuscript writing. **Adem Kara:** experiment, histopathology, immunohistochemistry, and western blot. **Elif Dalkilinc:** biochemical analysis. All authors contributed manuscript writing and approved the final manuscript.

Conflicts of Interest

The authors declare no conflicts of interest.

Data Availability Statement

The data that support the findings of this study are available from the corresponding author upon reasonable request.

References

1. R. C. Bone, "Gram-Negative Sepsis: A Dilemma of Modern Medicine," *Clinical Microbiology Reviews* 6, no. 1 (1993): 57–68.

2. M. Singer, C. S. Deutschman, C. W. Seymour, et al., "The Third International Consensus Definitions for Sepsis and Septic Shock (Sepsis-3)," *Journal of the American Medical Association* 315, no. 8 (2016): 801–810.

3. H. H. Dolin, T. J. Papadimos, X. Chen, and Z. K. Pan, "Characterization of Pathogenic Sepsis Etiologies and Patient Profiles: A Novel Approach to Triage and Treatment," *Microbiology Insights* 12 (2019): 1178636118825081.

4. P. E. Parsons, G. S. Worthen, E. E. Moore, R. M. Tate, and P. M. Henson, "The Association of Circulating Endotoxin With the Development of the Adult Respiratory Distress Syndrome," *American Review of Respiratory Disease* 140, no. 2 (1989): 294–301.

5. A. Maiese, A. Scatena, A. Costantino, et al., "Expression of MicroRNAs in Sepsis-Related Organ Dysfunction: A Systematic Review," *International Journal of Molecular Sciences* 23, no. 16 (2022): 9354.

6. A. J. Lewis, C. W. Seymour, and M. R. Rosengart, "Current Murine Models of Sepsis," *Surgical Infections* 17, no. 4 (2016): 385–393.

7. Y. Ozkanlar, M. Aktas, O. Kaynar, S. Ozkanlar, E. Kıreccı, and L. Yıldız, "Bovine Respiratory Disease in Naturally Infected Calves: Clinical Signs, Blood Gases and Cytokine Response," *Revue de Médecine Vétérinaire* 163, no. 3 (2012): 123–130.

8. Y. Ozkanlar, M. S. Aktas, M. Turkeli, et al., "Effects of Ramipril and Darbepoetin on Electromechanical Activity of the Heart in Doxorubicin-Induced Cardiotoxicity," *International Journal of Cardiology* 173, no. 3 (2014): 519–521.

9. M. Chopra, J. S. Reuben, and A. C. Sharma, "Acute Lung Injury: Apoptosis and Signaling Mechanisms," *Experimental Biology and Medicine (Maywood, N.J.)* 234, no. 4 (2009): 361–371.

10. C. Nedeva, J. Menassa, and H. Puthalakath, "Sepsis: Inflammation Is a Necessary Evil," *Frontiers in Cell and Development Biology* 7 (2019): 108.

11. X. Ding, N. A. Wilson, R. R. Redfield, 3rd, et al., "Oxidized-ATP Attenuates Kidney Allograft Rejection by Inhibiting T-Cell, B-Cell, and Macrophage Activity," *Kidney360* 1, no. 2 (2020): 106–114.

12. L. E. B. Savio, M. P. de Andrade, C. G. da Silva, and R. Coutinho-Silva, "The P2X7 Receptor in Inflammatory Diseases: Angel or Demon?," *Frontiers in Pharmacology* 9 (2018): 52.

13. P. A. Lang, D. Merkler, P. Funkner, et al., "Oxidized ATP Inhibits T-Cell-Mediated Autoimmunity," *European Journal of Immunology* 40, no. 9 (2010): 2401–2408.

14. C. A. Prauchner, "Oxidative Stress in Sepsis: Pathophysiological Implications Justifying Antioxidant Co-Therapy," *Burns* 43, no. 3 (2017): 471–485.

15. R. Xu, L. S. Yuan, Y. Q. Gan, et al., "Extracellular ATP Contributes to the Reactive Oxygen Species Burst and Exaggerated Mitochondrial Damage in D-Galactosamine and Lipopolysaccharide-Induced Fulminant Hepatitis," *International Immunopharmacology* 130 (2024): 111680.

16. M. D. Wewers and A. Sarkar, "P2X(7) Receptor and Macrophage Function," *Purinergic Signal* 5, no. 2 (2009): 189–195.

17. G. Burnstock, "P2X Ion Channel Receptors and Inflammation," *Purinergic Signal* 12, no. 1 (2016): 59–67.

18. G. Burnstock, "Purinergic Signalling: Therapeutic Developments," *Frontiers in Pharmacology* 8 (2017): 661.

19. S. Ozkanlar, N. Ulas, O. Kaynar, and E. Satici, "P2X7 Receptor Antagonist A-438079 Alleviates Oxidative Stress of Lung in LPS-Induced Septic Rats," *Purinergic Signal* 19 (2023): 699–707.

20. A. Kara and S. Ozkanlar, "Blockade of P2X7 Receptor-Mediated Purinergic Signaling With A438079 Protects Against LPS-Induced Liver Injury in Rats," *Journal of Biochemical and Molecular Toxicology* 37, no. 10 (2023): e23443.

21. M. L. Larrouyet-Sarto, A. S. Tamura, V. S. Alves, et al., "P2X7 Receptor Deletion Attenuates Oxidative Stress and Liver Damage in Sepsis," *Purinergic Signal* 16, no. 4 (2020): 561–572.

22. R. Kopp, A. Krautloher, A. Ramírez-Fernández, and A. Nicke, "P2X7 Interactions and Signaling – Making Head or Tail of It," *Frontiers in Molecular Neuroscience* 12 (2019): 183.

23. F. Albalawi, W. Lu, J. M. Beckel, J. C. Lim, S. A. McCaughey, and C. H. Mitchell, "The P2X7 Receptor Primes IL-1β and the NLRP3 Inflammasome in Astrocytes Exposed to Mechanical Strain," *Frontiers in Cellular Neuroscience* 11 (2017): 227.

24. J. M. Kahlenberg, K. C. Lundberg, S. B. Kertesy, Y. Qu, and G. R. Dubyak, "Potentiation of Caspase-1 Activation by the P2X7 Receptor Is Dependent on TLR Signals and Requires NF-kappaB-Driven Protein Synthesis," *Journal of Immunology* 175, no. 11 (2005): 7611–7622.

25. N. Arulkumaran, M. L. Sixma, S. Pollen, et al., "P2X(7) Receptor Antagonism Ameliorates Renal Dysfunction in a Rat Model of Sepsis," *Physiological Reports* 6, no. 5 (2018): e13622.

26. I. Higuera-Ciapara, L. Félix-Valenzuela, and F. M. Goycoolea, "Astaxanthin: A Review of Its Chemistry and Applications," *Critical Reviews in Food Science and Nutrition* 46, no. 2 (2006): 185–196.

27. Y. Kishimoto, H. Yoshida, and K. Kondo, "Potential Anti-Atherosclerotic Properties of Astaxanthin," *Marine Drugs* 14, no. 2 (2016): 35.

28. P. Alugoju, V. K. D. Krishna Swamy, N. V. A. Anthikapalli, and T. Tencomnao, "Health benefits of astaxanthin against age-related diseases of multiple organs: A comprehensive review," *Critical Reviews in Food Science and Nutrition* 63 (2022): 1–66.

29. S. Wang and X. Qi, "The Putative Role of Astaxanthin in Neuroinflammation Modulation: Mechanisms and Therapeutic Potential," *Frontiers in Pharmacology* 13 (2022): 916653.

30. M. Wang, X. Deng, Y. Xie, and Y. Chen, "Astaxanthin Attenuates Neuroinflammation in Status Epilepticus Rats by Regulating the ATP-P2X7R Signal," *Drug Design, Development and Therapy* 14 (2020): 1651–1662.

31. J. Bi, R. Cui, Z. Li, C. Liu, and J. Zhang, "Astaxanthin Alleviated Acute Lung Injury by Inhibiting Oxidative/Nitrative Stress and the Inflammatory Response in Mice," *Biomedicine & Pharmacotherapy* 95 (2017): 974–982.

32. L. Luo, F. Huang, S. Zhong, R. Ding, J. Su, and X. Li, "Astaxanthin Attenuates Ferroptosis via Keap1-Nrf2/HO-1 Signaling Pathways in LPS-Induced Acute Lung Injury," *Life Sciences* 311, no. Pt A (2022): 121091.

33. Z. Zou, Q. Wang, M. Zhou, et al., "Protective Effects of P2X7R Antagonist in Sepsis-Induced Acute Lung Injury in Mice via Regulation of circ_0001679 and circ_0001212 and Downstream Pln, Cdh2, and Nprl3 Expression," *Journal of Gene Medicine* 22, no. 12 (2020): e3261.

34. H. Liu, J. Hao, C. Wu, et al., "Eupatilin Alleviates Lipopolysaccharide-Induced Acute Lung Injury by Inhibiting Inflammation and Oxidative Stress," *Medical Science Monitor* 25 (2019): 8289–8296.

35. W. Sun, Z. Cheng, H. Chen, G. Lin, and H. Chen, "Tetrahydropyrimidines, ZL-5015 Alleviated Lipopolysaccharide (LPS)-Induced Acute Pneumonia in Rats by Activating the NRF-2/HO-1 Pathway," *Medical Science Monitor* 26 (2020): e924482.

36. M. X. Chang and F. Xiong, "Astaxanthin and Its Effects in Inflammatory Responses and Inflammation-Associated Diseases: Recent Advances and Future Directions," *Molecules* 25, no. 22 (2020): 5342.

37. X. Yang, A. L. Guo, Y. P. Pang, et al., "Astaxanthin Attenuates Environmental Tobacco Smoke-Induced Cognitive Deficits: A Critical Role of p38 MAPK," *Marine Drugs* 17, no. 1 (2019): 24.

38. G. Matute-Bello, C. W. Frevert, and T. R. Martin, "Animal Models of Acute Lung Injury," *American Journal of Physiology. Lung Cellular and Molecular Physiology* 295, no. 3 (2008): L379–L399.

39. J. I. Fortea, M. Puerto, C. Fernández-Mena, et al., "Sevoflurane Versus Ketamine+Diazepam Anesthesia for Assessing Systemic and Hepatic Hemodynamics in Rats With Non-Cirrhotic Portal Hypertension," *PLoS One* 15, no. 5 (2020): e0233778.

40. J. C. Wrba, L. Lupu, S. Braumüller, et al., "Effects of Anesthesia With Sevoflurane on Outcome Parameters in Murine Experimental Studies," *European Journal of Trauma and Emergency Surgery* 50 (2024): 3281–3287.

41. M. R. Passmore, L. Byrne, N. G. Obonyo, et al., "Inflammation and Lung Injury in an Ovine Model of Fluid Resuscitated Endotoxemic Shock," *Respiratory Research* 19, no. 1 (2018): 231.

42. J. A. Englert, C. Bobba, and R. M. Baron, "Integrating Molecular Pathogenesis and Clinical Translation in Sepsis-Induced Acute Respiratory Distress Syndrome," *Journal of Clinical Investigation Insight* 4, no. 2 (2019): e124061.

43. F. B. Santos, L. K. Nagato, N. M. Boechem, et al., "Time Course of Lung Parenchyma Remodeling in Pulmonary and Extrapulmonary Acute Lung Injury," *Journal of Applied Physiology* 100, no. 1 (2006): 98–106.

44. A. Donoso, J. González-Durán, A. A. Muñoz, P. A. González, and C. Agurto-Muñoz, "Therapeutic Uses of Natural Astaxanthin: An Evidence-Based Review Focused on Human Clinical Trials," *Pharmacological Research* 166 (2021): 105479.

45. X. Que, M. Y. Hung, C. Yeang, et al., "Oxidized Phospholipids Are Proinflammatory and Proatherogenic in Hypercholesterolaemic Mice," *Nature* 558, no. 7709 (2018): 301–306.

46. I. P. Pratomo, A. Tedjo, D. R. Noor, and Rosmalena, "Differentially Expressed Genes Analysis in the Human Small Airway Epithelium of Healthy Smokers Shows Potential Risks of Disease Caused by Oxidative Stress and Inflammation and the Potentiality of Astaxanthin as an Anti-Inflammatory Agent," *International Journal of Inflammation* 2023 (2023): 4251299.

47. H. Tang, Y. Zhang, Q. Wang, et al., "Astaxanthin Attenuated Cigarette Smoke Extract-Induced Apoptosis via Decreasing Oxidative DNA Damage in Airway Epithelium," *Biomedicine & Pharmacotherapy* 167 (2023): 115471.

48. Y. Yin, N. Xu, T. Qin, et al., "Astaxanthin Provides Antioxidant Protection in LPS-Induced Dendritic Cells for Inflammatory Control," *Marine Drugs* 19, no. 10 (2021): 534.

49. X. Dong, D. Li, Z. Fang, C. Zhang, J. Wang, and X. Wan, "Astaxanthin Alleviates Lipopolysaccharide-Induced Acute Lung Injury by Suppressing Ferroptosis," *Food & Function* 14, no. 13 (2023): 6115–6127.

50. E. A. Townsend, A. Guadarrama, L. Shi, E. Roti Roti, and L. C. Denlinger, "P2X(7) Signaling Influences the Production of Pro-Resolving and Pro-Inflammatory Lipid Mediators in Alveolar Macrophages Derived From Individuals With Asthma," *American Journal of Physiology. Lung Cellular and Molecular Physiology* 325, no. 4 (2023): L399–L410.

51. E. Nuka, K. Ohnishi, J. Terao, and Y. Kawai, "ATP/P2X7 Receptor Signaling as a Potential Anti-Inflammatory Target of Natural Polyphenols," *PLoS One* 13, no. 9 (2018): e0204229.

52. A. Mishra, Y. Guo, L. Zhang, et al., "A Critical Role for P2X7 Receptor-Induced VCAM-1 Shedding and Neutrophil Infiltration During Acute Lung Injury," *Journal of Immunology* 197, no. 7 (2016): 2828–2837.

53. F. M. Munoz, P. A. Patel, X. Gao, et al., "Reactive Oxygen Species Play a Role in P2X7 Receptor-Mediated IL-6 Production in Spinal Astrocytes," *Purinergic Signal* 16, no. 1 (2020): 97–107.

54. N. Riteau, P. Gasse, L. Fauconnier, et al., "Extracellular ATP Is a Danger Signal Activating P2X7 Receptor in Lung Inflammation and Fibrosis," *American Journal of Respiratory and Critical Care Medicine* 182, no. 6 (2010): 774–783.

55. S. Janho Dit Hreich, T. Juhel, S. Leroy, et al., "Activation of the P2RX7/IL-18 Pathway in Immune Cells Attenuates Lung Fibrosis," *eLife* 12 (2024): RP88138.

56. C. Jiao, H. Zhang, H. Li, et al., "Caspase-3/GSDME Mediated Pyroptosis: A Potential Pathway for Sepsis," *International Immunopharmacology* 124, no. Pt B (2023): 111022.

57. H. Zeng, X. Kong, H. Peng, et al., "Apoptosis and Bcl-2 Family Proteins, Taken to Chronic Obstructive Pulmonary Disease," *European Review for Medical and Pharmacological Sciences* 16, no. 6 (2012): 711–727.

58. T. Liu, L. Zhang, D. Joo, and S. C. Sun, "NF-κB Signaling in Inflammation," *Signal Transduction and Targeted Therapy* 2 (2017): 17023.

59. N. F. Oliveira, M. Monteiro, N. S. Mainieri, et al., "P2Y(2)-P2X7 Receptors Cross-Talk in Primed Mesenteric Endothelial Cells Upregulates NF-κB Signaling Favoring Mononuclear Cell Adhesion in Schistosomiasis," *Frontiers in Immunology* 14 (2023): 1328897.

60. Y. Liu, Y. Xiao, and Z. Li, "P2X7 Receptor Positively Regulates MyD88-Dependent NF-κB Activation," *Cytokine* 55, no. 2 (2011): 229–236.

61. M. Gu, A. B. Zheng, J. Jin, et al., "Cardioprotective Effects of Genistin in Rat Myocardial Ischemia-Reperfusion Injury Studies by Regulation of P2X7/NF-κB Pathway," *Evidence-Based Complementary and Alternative Medicine* 2016 (2016): 5381290.

62. S. R. Wann, H. R. Lo, Y. T. Chang, J. B. Liao, Z. H. Wen, and P. L. Chi, "P2X7 Receptor Blockade Reduces Pyroptotic Inflammation and Promotes Phagocytosis in *Vibrio vulnificus* Infection," *Journal of Cellular Physiology* 238, no. 10 (2023): 2316–2334.

63. Z. Cai, J. Liu, H. Bian, J. Cai, and G. Zhu, "Suppression of P2X7/NF-κB Pathways by Schisandrin B Contributes to Attenuation of Lipopolysaccharide-Induced Inflammatory Responses in Acute Lung Injury," *Archives of Pharmacal Research* 39, no. 4 (2016): 499–507.

64. J. Dagvadorj, K. Shimada, S. Chen, et al., "Lipopolysaccharide Induces Alveolar Macrophage Necrosis via CD14 and the P2X7 Receptor Leading to Interleukin-1α Release," *Immunity* 42, no. 4 (2015): 640–653.

65. S. Davinelli, L. Saso, F. D'Angeli, V. Calabrese, M. Intrieri, and G. Scapagnini, "Astaxanthin as a Modulator of Nrf2, NF-κB, and Their Crosstalk: Molecular Mechanisms and Possible Clinical Applications," *Molecules* 27, no. 2 (2022): 502.

66. S. Fakhri, F. Abbaszadeh, L. Dargahi, and M. Jorjani, "Astaxanthin: A Mechanistic Review on Its Biological Activities and Health Benefits," *Pharmacological Research* 136 (2018): 1–20.

67. J. Cheng and A. Eroglu, "The Promising Effects of Astaxanthin on Lung Diseases," *Advances in Nutrition* 12, no. 3 (2021): 850–864.

68. L. Li, A. Alimu, X. Zhong, et al., "Protective Effect of Astaxanthin on Tuberculosis-Associated Inflammatory Lung Injury," *Experimental Biology and Medicine* 248, no. 4 (2023): 293–301.

69. K. S. Liao, C. L. Wei, J. C. Chen, et al., "Astaxanthin Enhances Pemetrexed-Induced Cytotoxicity by Downregulation of Thymidylate Synthase Expression in Human Lung cancer Cells," *Regulatory Toxicology and Pharmacology* 81 (2016): 353–361.

70. L. Zhu, H. Wu, Z. Ma, D. Dong, Z. Yang, and J. Tian, "Astaxanthin Ameliorates Lipopolysaccharide-Induced Acute Lung Injury via

Inhibition of Inflammatory Reactions and Modulation of the SOCS3/JAK2/STAT3 Signaling Pathways in Mice," *Food & Function* 13, no. 22 (2022): 11638–11651.

71. X. Wu, Q. Kong, L. Zhan, Z. Qiu, Q. Huang, and X. Song, "TIPE2 Ameliorates Lipopolysaccharide-Induced Apoptosis and Inflammation in Acute Lung Injury," *Inflammation Research* 68, no. 11 (2019): 981–992.

72. J. T. Opferman and A. Kothari, "Anti-Apoptotic BCL-2 Family Members in Development," *Cell Death and Differentiation* 25, no. 1 (2018): 37–45.